Title

Coordination Characteristics of Uranyl BBP Complexes: Insights from an Electronic Structure Analysis

Permalink

https://escholarship.org/uc/item/99p3s3nz

Journal

ACS Omega, 2(3)

ISSN

2470-1343

Authors

Pemmaraju, Chaitanya Das

Copping, Roy

Smiles, Danil E

et al.

Publication Date

2017-03-31

DOI

10.1021/acsomega.6b00459

Copyright Information

Peer reviewed

Coordination Characteristics of Uranyl BBP Complexes: Insights from an Electronic Structure Analysis

Chaitanya Das Pemmaraju,*,[†] Roy Copping,[‡] Danil E. Smiles,[‡] David K. Shuh,[‡] Niels Grønbech-Jensen,[⊥] David Prendergast,[§] and Andrew Canning[∥]

[†]Chemical and Materials Sciences Divisions, [‡]Chemical Sciences Division, The Glenn T. Seaborg Center, [§]The Molecular Foundry, [∥]Computational Research Division, Lawrence Berkeley National Laboratory, Berkeley, California 94720, United States
[⊥]Department of Applied Science, University of California, Davis, California 95616, United States

ABSTRACT: Organic ligand complexes of lanthanide/actinide ions have been studied extensively for applications in nuclear fuel storage and recycling. Several complexes of 2,6-bis(2-benzimidazyl)pyridine (H2BBP) featuring the uranyl moiety have been reported recently, and the present study investigates the coordination characteristics of these complexes using density functional theory-based electronic structure analysis. In particular, with the aid of several computational models, the nonplanar equatorial coordination about uranyl, observed in some of the compounds, is studied and its origin traced to steric effects.
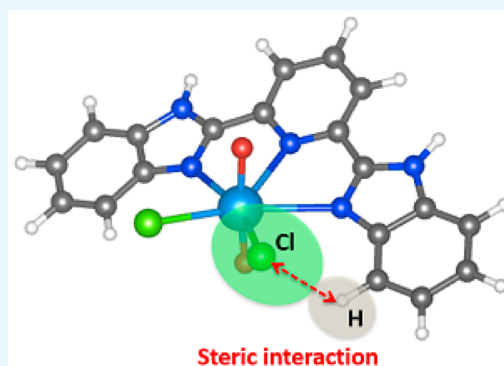
INTRODUCTION

It is essential to understand the behavior of actinide complexes for the development of separation technologies and future nuclear fuel recycling processes.[1] Organic ligands, which coordinate to lanthanides/actinides, have been studied extensively[2] and will be a key element in the management and long-term storage of nuclear waste. In this context, the tridentate N-donor ligand 2,6-bis(2-benzimidazyl)pyridine (H$_2$BBP), shown schematically in Figure 1, has been studied in the past as a low-valent actinide sequestering agent and as a sensitizer for lanthanide luminescence.[3−9] We have previously reported the experimental synthesis and spectroscopic characterization of a series of uranyl ($\{UO_2\}^{2+}$) complexes featuring the BBP ligand and its derivatives.[10,11] Interestingly, crystallographic characterization of the complexes revealed nonplanarity in the equatorial ligand coordination structure about the uranyl moiety and a modulation of the nonplanarity with changing ligand character, all without significant structural changes in the uranyl moiety. Structural distortions of uranyl complexes have been examined extensively, and much of the focus has been upon the uranyl moiety itself.[12−15] Altering both the steric and electronic characteristics of the equatorial ligands has been shown to play a role in changing the U=O bond lengths of the ($\{UO_2\}^{2+}$) structural unit as well as opening up new avenues for reactivity.[16,17] There has also been interest in distorting the dioxo O−U−O bond angle from its typical linear arrangement.[18−22] Recently, Hayton and co-workers reported a series of uranyl complexes with macrocyclic ligands, whose steric constraints push the O−U−O bond angle slightly away from its desired linear arrangement.[22] Distortion of the equatorial ligands has also been seen previously in other uranyl

complexes.[22−24] For example, Berthet and co-workers reported a variety of uranyl complexes featuring different N-donor ligands, including $[(UO_2)(terpy)(OTf)_2]$ (terpy = 2,6-bis(2-pyridyl)-pyridine) and $[U(phen)_3][OTf]_2$ (phen = 1,10-phenanthroline), which both exhibit a significant deviation from planarity.[24]

The aim of this study is to investigate in detail the coordination characteristics of BBP−uranyl complexes through first-principles theoretical simulations and to determine the origin of the nonplanarity of the equatorial ligands, either steric or electronic. To this end, a series of computational experiments are carried out, which clarify the relationship between ligand character and nonplanarity.

The three complexes, $[(UO_2)(H_2BBP)Cl_2]$ (**1**), $[(UO)_2(HBBP)(Py)Cl]$ (**2**), and $[(UO_2)(BBP)(Py)_2]$ (**3**), that were experimentally synthesized and form the primary subjects of this investigation are shown in Figure 2. The complexes have similar BBP ligands, which provide three coordinating bonds, but differ in the character of the two additional ligands that complete the pentagonal equatorial coordination structure around the uranyl moiety. Compound **1** has two Cl$^-$ groups, compound **2** has one Cl$^-$ and one pyridine, whereas compound **3** has two pyridines as the additional ligands. There are also concomitant differences in the charge state of the BBP ligand. As shown in Figure 2, N4 and N5 on the BBP ligand are protonated in compound **1** and are both deprotonated in **3**. In **2**, N5, which is on the side of the pyridine attachment, is protonated, whereas N4 is not. In terms of coordination, **1** and **2**
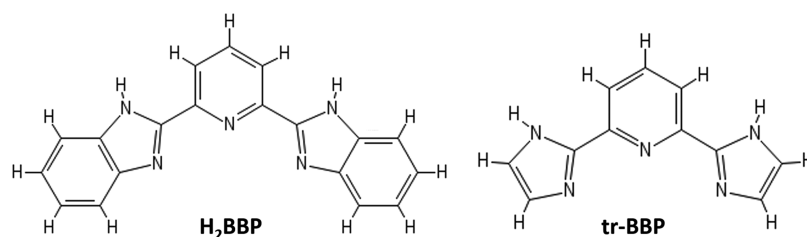
Figure 1. Schematics of the organic ligands used in this study. [Left] 2,6-Bis(2-benzimidazyl)pyridine (H$_2$BBP); [right] smaller ligand obtained from H$_2$BBP by truncating the benzene rings of the benzimidazole groups.
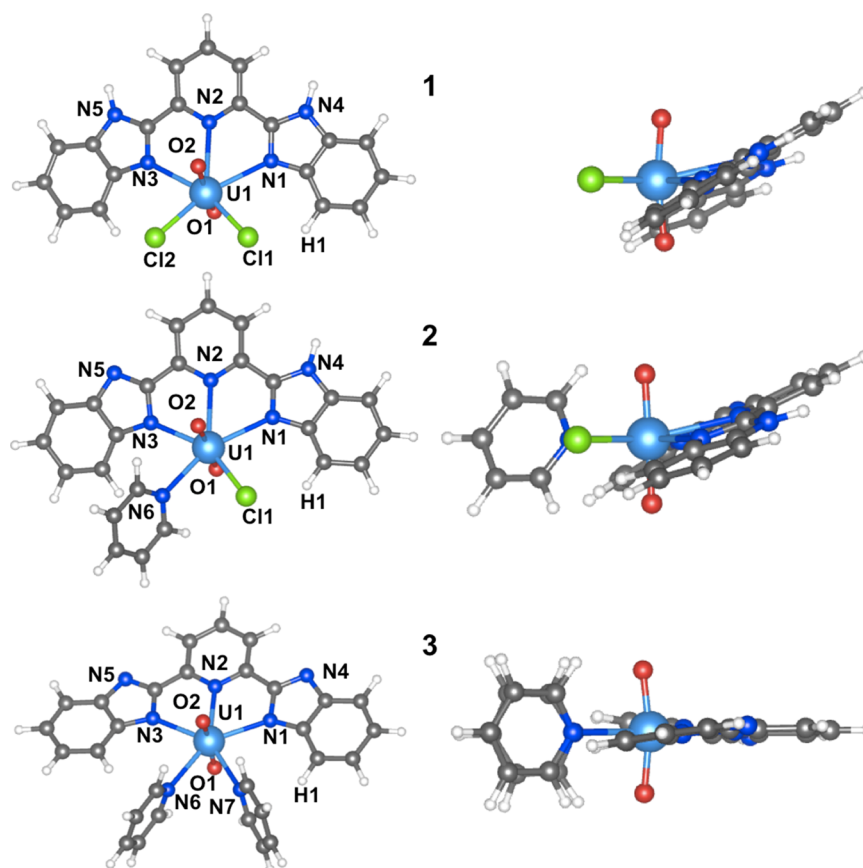

Figure 2. Labeling and structure of three BBP–uranyl complexes. Side views are shown on the right side. Compounds **1** and **2** show the distinct asymmetric uranyl structure with respect to pyridine ligand planes. Color code: U, light blue; N, dark blue; O, red; Cl, green; C, gray; H, white.

Table 1. GGA-Optimized Structural Parameters for Isolated Molecules of Compounds 1–3 Are Compared to Experimental Molecular Crystal Data[a]

compound **1**			compound **2**			compound **3**		
bond/angle	expt.	GGA	bond/angle	expt.	GGA	bond/angle	expt.	GGA
U–O1	1.766	1.825	U–O1	1.762	1.821	U–O1	1.768	1.827
U–O2	1.772	1.827	U–O2	1.773	1.822	U–O2	1.768	1.827
U–N1	2.556	2.707	U–N1	2.593	2.646	U–N1	2.501	2.513
U–N2	2.606	2.754	U–N2	2.573	2.614	U–N2	2.519	2.489
U–N3	2.581	2.705	U–N3	2.533	2.522	U–N3	2.501	2.512
U–Cl1	2.661	2.603	U–N6	2.554	2.586	U–N6	2.538	2.642
U–Cl2	2.692	2.605	U–Cl1	2.685	2.637	U–N7	2.538	2.642
∠O1 = U = O2	178.1	169.7	∠O1 = U = O2	176.53	177.2	∠O1 = U = O2	176.2	169.5
∠N1–N2–N3	113.0	115.3	∠N1–N2–N3	114.43	113.8	∠N1–N2–N3	114.94	113.8
∠Eq./N1N2N3	30.90	28.4	∠Eq./N1N2N3	13.20	24.3	∠Eq./N1N2N3	3.5	2.1

[a]Equatorial planes are generated by sets of three points, namely, Cl1–U–Cl2 in compound **1**, Cl1–U–N6 in compound **2**, and N6–U–N7 in compound **3** (see Figure 2). Units for distances and angles are angstroms and degrees, respectively.

exhibit distinct noncoplanarity with the equatorial plane compared to **3**, which is coplanar about the equatorial plane and symmetric under reflection. One of the main objectives of the current study is to determine whether electronic or steric effects drive the observed coordination structure differences in these complexes. A density functional theory (DFT)-based analysis of the crystal structures of the three molecular complexes, **1**−**3**, has been reported previously.[10] However, as will be shown later, crystal packing has very little effect on the interesting structural differences related to nonplanarity about the uranyl. Additionally, some of the complexes we simulate to investigate trends in bonding and nonplanarity have not been synthesized experimentally, and because the molecular crystals of these systems often depend on incorporated solvent units, trying to predict their crystalline structures from first-principles simulations would distract from the main focus of this work. Therefore, in this study, we investigate the intrinsic structural characteristics of the isolated molecular units of BBP−uranyl complexes free from crystal packing effects.

■ RESULTS AND DISCUSSION

Relevant bond lengths and bond angles extracted from optimized geometries of the isolated complexes are compared to experimental molecular crystal values, as summarized in Table 1. We have shown previously[10] that generalized gradient approximation (GGA)-optimized structural parameters of molecular crystals agree reasonably well with the experiment with errors within the 3% range. In the case of isolated complexes, we find slightly larger differences, with bond lengths typically longer by 3−5% compared to those of experimental crystal structures, and we attribute this to the absence of the crystalline environment in the calculations. However, the utility of the isolated molecular calculations is that they enable us to identify trends in the structural properties that are intrinsic to the complexes rather than driven by crystal packing. For instance, the experimentally observed trend that the BBP N−U bond lengths get progressively shorter going from **1** to **3** is reproduced for the isolated complexes. Accordingly, as can be inferred from Table 1, the average calculated BBP N−U bond length decreases from 2.722 to 2.505 Å going from **1** to **3**. Meanwhile, the crystalline O═U═O bond angles deviate from 180° by an increasing degree going from **1** to **3**, but this trend is not observed in the simulated structures of the isolated complexes. This is because the O═U═O bond angle is significantly affected by crystal packing and DFT simulations reproduce the observed trend in crystals.[10] Meanwhile, the U═O bond lengths do not change significantly across the three complexes in both the experimental and theoretical structures.

To better understand the origin of the observed nonplanarity in **1** and **2**, we investigated several potential driving factors, such as crystal packing, ligand character, and steric hindrance. The degree of nonplanarity about the uranyl is quantified by first defining an equatorial plane in each complex built by sets of three points: (U1, Cl1, Cl2) in **1**, (U1, Cl1, N6) in **2**, and (U1, N6, N7) in **3**. The angle between the equatorial plane and a plane formed by the BBP N sites (N1, N2, N3) shows how much the uranyl is elevated with respect to the plane of the BBP, yielding the degree of nonplanarity. As shown in Table 1, compound **1** shows the highest angle, whereas compound **3** is virtually flat and symmetric, in both the experiments and computations. Complex **2** shows an intermediate nonplanar angle between compounds **1** and **3**.

The realization of a nonplanar configuration in isolated units of complexes **1** and **2** suggests that it is an intrinsic feature of the complexes themselves and not a result of crystal packing effects. However, given the structural complexity of these compounds, we still need to verify the energetic stability of the nonplanar structures with respect to planar motifs. To this end, we consider a model unit of complex **1** in a supercell geometry, with the structure of the model initially configured so that all of the equatorial ligands form a plane as shown in Figure 3. We then
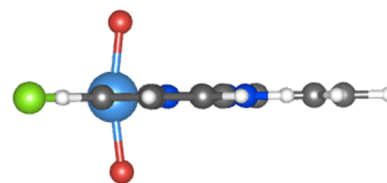

Figure 3. Side view of model complex **1** with all of the BBP ligand atoms constrained to lie in the equatorial plane formed by the Cl1−U−Cl2 group of atoms.

carry out a constrained structural optimization whereby all of the atoms of the BBP ligand are constrained to lie in the Cl1−U−Cl2 plane during the optimization. Once all of the forces in this planar structure fall below 0.01 eV/Å, we release the previously imposed constraint and allow all of the atomic positions to further relax until all of the forces are smaller than 0.001 eV/Å. Thus, we find that a planar configuration with almost no forces acting on the atoms can be realized in the calculation even though its energy is 0.124 eV higher than that of the optimized nonplanar configuration, suggesting that the planar configuration is at best a local minimum. A vibrational analysis of the planar structure confirms the instability through an imaginary low-frequency (26.4 cm^{-1}) vibrational mode with an out-of-plane displacement of the entire $\{UO_2\}^{2+}$ unit relative to the BBP ligand. This establishes that the nonplanar geometry is indeed the intrinsically stable minimum-energy configuration of **1** and not a result of crystal packing. Interestingly, the geometric parameters of the optimized planar and nonplanar configurations of the isolated complex, **1**, provide some insight into the role of sterics (see Table 2). We find that in the out-of-plane configuration, BBP *N*-uranyl bond lengths are shorter on average by ∼0.034 Å, the U−N1 and U−N2 bonds being significantly shorter, and ∠N1−N2−N3 of the BBP ligand at 115.3° is also smaller by 2.9° compared to that in the in-plane configuration. In contrast, ∠Cl1−U−Cl2 is smaller by 5.6° and the Cl1−H1 and Cl2−H2 distances are 9.5% shorter in the planar geometry. Thus, accommodating $\{UO_2\}^{2+}$ in the plane of the BBP ligand requires a more open ∠N1−N2−N3, longer BBP *N*-uranyl bonds, and a narrower ∠Cl1−U−Cl2, all of which suggest steric interaction in the equatorial plane between the Cl$^-$ ions and the nearby H groups on the benzimidazole rings of BBP. Conversely, being out-of-plane and thereby increasing the Cl1−H1 and Cl2−H2 distances not only allows the uranyl to strengthen its bonding to the BBP ligand but also allows the latter to achieve an unstrained ∠N1−N2−N3 that is similar to that found in complexes **2** and **3**. These findings point to the steric interaction between the Cl$^-$ ions and the H sites on the outer benzimidazole groups as potentially driving the nonplanarity.

To further investigate this, we consider the effect of substituting the Cl$^-$ ligands in complex **1** with other halide ligands characterized by different ionic radii and electronegativities. We note that in contrast to when the Cl$^-$ ligands

Table 2. GGA-Optimized Structural Parameters for an Isolated Molecule of Complex 1 Are Compared to Those of a Constrained Model of Complex 1 Wherein the Structure Is Optimized While Forcing All the BBP Ligand Atoms To Lie in the Same Equatorial Plane Defined by the Three Points, Cl1−U−Cl2 (See Figure 3)[a]

bond/angle	complex 1	planar complex 1
U−O1	1.825	1.824
U−O2	1.827	1.824
U−N1	2.707	2.751
U−N2	2.754	2.765
U−N3	2.705	2.752
U−Cl1	2.603	2.607
U−Cl2	2.605	2.606
Cl1⋯H1	2.592	2.322
Cl2⋯H2	2.542	2.324
∠N1−N2−N3	115.3	118.2
∠N1−U−N3	118.9	122.5
∠Cl1−U−Cl2	84.2	78.6
∠Eq./N1N2N3	28.4	0.0

[a]Units for distances and angles are angstroms and degrees, respectively.

are replaced by pyridine ligands the substitution of Cl⁻ by other halides leaves the formal charge on the BBP ligand unchanged, enabling us to vary the properties of one set of ligands, that is, the halides whereas leaving the properties of the BBP ligand nominally unchanged. In Table 3, we present GGA-optimized geometric parameters for a series of molecules derived from complex 1 by substituting Cl⁻ with F⁻ through I⁻ (see Figure 4). We find that the out-of-plane angle increases monotonically with increasing ionic radius (r_{ion}) of the halide ligands (indicated by labels $\alpha1$ and $\alpha2$), going from an almost planar structure for F⁻ to a nonplanar angle of 39.9° in the case of I⁻. Additionally, ∠$\alpha1$−U−$\alpha2$ is also seen to decrease monotonically from F⁻ to I⁻ with an overall change of 5%. In particular, as shown in Table 3, (r_{ion} + 0.9 Å) is seen to be a good approximation to the distance between each halide ion and the nearest H site on the BBP benzimidazole groups across all of the halide ligand complexes. This suggests that in these complexes the $\alpha1$−uranyl−$\alpha2$ moiety moves out of the BBP plane and simultaneously ∠$\alpha1$−U−$\alpha2$

reduces until the halide to benzimidazole H distance reaches approximately (r_{ion} + 0.9 Å). An effective radius of 0.9 Å is therefore indicated for H groups in their interaction with halide ions. Meanwhile, the U−N1 and U−N3 bond lengths show neither significant variation nor a systematic trend across the halide-substituted series, whereas the U−N2 bond length actually decreases slightly going from F⁻ to I⁻. This is in contrast to complexes 2 and 3 where the reduced nonplanar angle is also accompanied by reduced U−N1, U−N2, and U−N3 distances relative to 1. Thus, we can infer that once the halide−benzimidazole H steric interaction is accommodated through nonplanarity, the BBP N-uranyl bond lengths are modulated primarily by the effective charge state of the BBP ligand. A similar computational experiment as described before in the case of complex 1, with structures generated by initially enforcing perfect planarity of all atoms in the BBP ligand and the $\alpha1$−U−$\alpha2$ group, indicates that the optimized planar structures are higher in energy than the corresponding fully unconstrained equilibrium structures by 0.025, 0.124, 0.197, and 0.316 eV in the F⁻-, Cl⁻-, Br⁻-, and I⁻-substituted complexes, respectively. A vibrational frequency analysis further indicates that such structures are unstable with respect to a motion of the $\alpha1$−U−$\alpha2$ moiety out of the plane of the BBP ligand. Soft imaginary frequency modes corresponding to this out-of-plane motion are obtained at 18, 26, 29, and 36 cm⁻¹ for the F⁻-, Cl⁻-, Br⁻-, and I⁻-substituted complexes, respectively. We note in this instance that both the energy difference between the perfectly planar and unconstrained structures and the magnitude of the unstable mode energies increase monotonically with the halide ligand size. Interestingly, for F⁻, although a weakly unstable mode for out-of-plane motion of F⁻−U−F⁻ is detected in the perfectly planar structure, in practice, the F⁻ complex assumes its lower energy equilibrium geometry through a slight buckling of the BBP ligand itself rather than such an out-of-plane motion.

Having established that for a given N-donor ligand, that is, BBP, reducing the ionic radius of the equatorial halide ligands leads to a reduced out-of-plane angle, we next investigated if for a given halide ligand, reducing the effective size of the N-donor ligand leads to a similar trend. We reason that if steric hindrance is the primary driver of nonplanarity then the effect should be similar whether it is the size of the halide ligands or the N-donor

Table 3. GGA-Optimized Structural Parameters for Isolated Molecular Units Derived from Complex 1 by Different Halide Ligand Substitutions Are Compared[a]

bond/angle	F [r_{ion} = 1.19 Å]	Cl [r_{ion} = 1.67 Å]	Br [r_{ion} = 1.82 Å]	I [r_{ion} = 2.06 Å]
U−O1	1.838	1.825	1.822	1.821
U−O2	1.840	1.827	1.827	1.826
U−N1	2.668	2.707	2.683	2.684
U−N2	2.780	2.754	2.748	2.735
U−N3	2.671	2.705	2.681	2.683
U−$\alpha1$	2.137	2.603	2.776	3.022
U−$\alpha2$	2.137	2.605	2.777	3.020
$\alpha1$⋯H1	2.071 (2.09)	2.592 (2.57)	2.795 (2.72)	3.001 (2.96)
$\alpha2$⋯H2	2.068 (2.09)	2.542 (2.57)	2.796 (2.72)	3.013 (2.96)
∠N1−N2−N3	115.2	115.3	113.2	113.1
∠N1−U−N3	121.4	118.9	116.4	116.1
∠$\alpha1$−U−$\alpha2$	87.7	84.2	85.1	83.3
∠Eq./N1N2N3	1.7	28.4	36.5	39.9

[a]In column 1, $\alpha1$ and $\alpha2$ represent the placeholders for the two halide ligand sites (see Figure 4). The equatorial planes are generated by sets of three points, namely, $\alpha1$, U, and $\alpha2$. Units for distances and angles are angstroms and degrees, respectively. The numbers in parentheses indicate (r_{ion} + 0.9 Å).
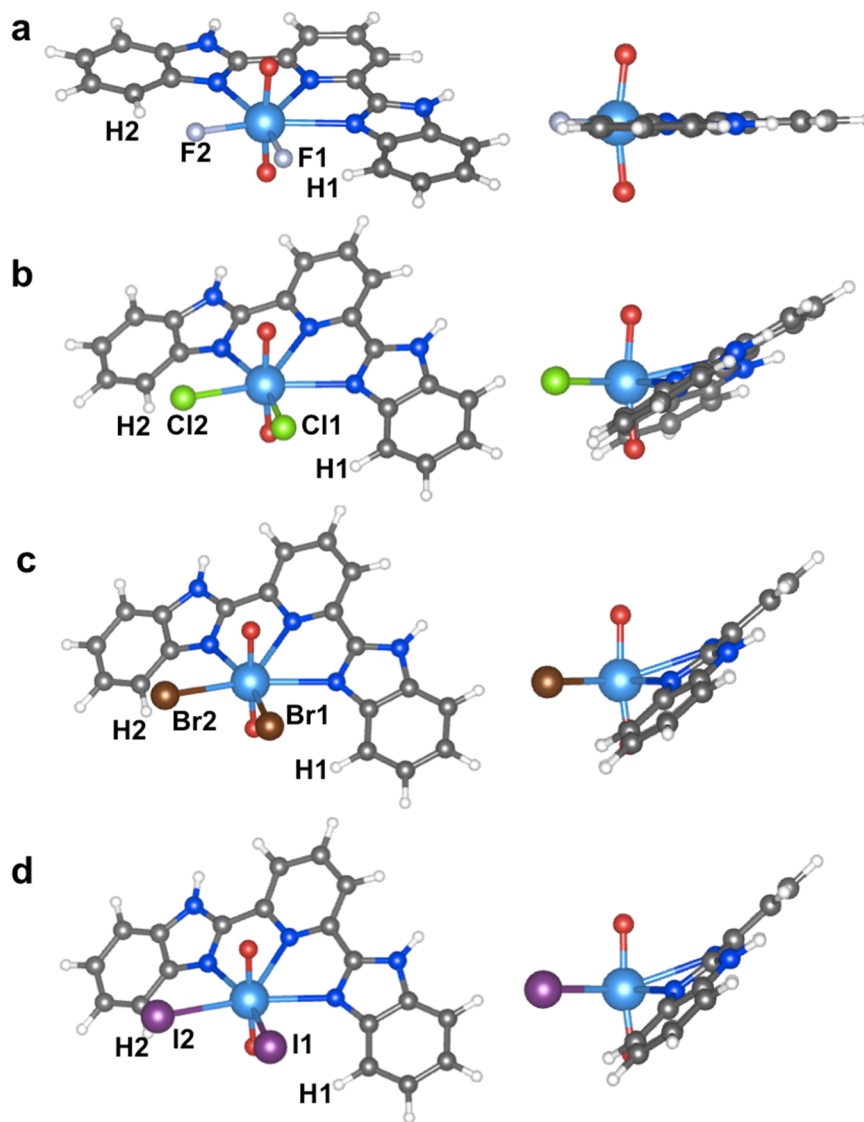
Figure 4. Structural models of isolated molecular units derived from complex 1 by incorporating different halide ligand substitutions; (a) F⁻, (b) Cl⁻, (c) Br⁻, and (d) I⁻; are shown. Side views of the complexes are shown on the right. For those atoms not explicitly labeled, the same labeling convention as used in Figure 2 is followed.

ligand that is reduced. Accordingly, we truncated the outer benzene rings of the benzimidazole groups on the BBP ligand to obtain a smaller pi-conjugated ligand (see Figure 1) such that for a given nonplanar angle, the H atoms on the imidazole rings of this ligand are farther away from the halide ions. This truncated BBP (tr-BBP) ligand has the same nominal charge state as that of the unmodified BBP ligand. We constructed four modified complexes featuring the tr-BBP and F⁻, Cl⁻, Br⁻, and I⁻ ligands as shown in Figure 5 and optimized their geometries. We find that for each type of halide ion the degree of nonplanarity with the tr-BBP ligand is significantly smaller than that with the original BBP ligand as is evident from the nonplanar angles reported in Table 4. Furthermore, we see that in the case of the larger halide ions where perfect planarity is not attained, the final distance between the halide ion and the nearest H atom on tr-BBP is similar to the corresponding value observed in the case of the unmodified BBP ligand (see Table 3). For Cl⁻, Br⁻, and I⁻, (r_{ion} + 0.9 Å) is once again a good predictor of the optimized halide to H group distance, whereas for the smaller F⁻ ion where planarity is reached, this distance is larger than (r_{ion} + 0.9 Å).

Finally, as before, we find a monotonic decrease of $\angle \alpha 1 - U - \alpha 2$ and the U−N2 bond length with increasing r_{ion}, whereas the U−N1 and U−N3 bond lengths show a weak but opposite trend. $\angle$N1−N2−N3 also show a weak monotonically increasing trend across the series but with values that are comparable to those obtained with the full BBP ligand. Weaker trends are also apparent in perfectly planar analogues of the tr-BBP complexes where, as before, planarity of all atoms in the tr-BBP ligand and the $\alpha 1 - U - \alpha 2$ moiety is initially enforced. We find that the optimized planar structures are higher in energy relative to the equilibrium structures by 0.058, 0.085, 0.061, and 0.064 eV, respectively, for the F⁻, Cl⁻, Br⁻, and I⁻ ligand complexes. Interestingly, a vibrational analysis of the planar structures does not yield unstable modes corresponding to a clear out-of-plane motion of the $\alpha 1 - U - \alpha 2$ moiety except in the case of the F⁻ complex. This suggests that the planar Cl⁻-, Br⁻-, and I⁻-substituted tr-BBP−uranyl complexes represent higher energy local minima, whereas the planar F⁻ complex, with more compact U−N1 and U−N3 bonds and a smaller $\angle$N1−N2−N3, is weakly unstable. Despite subtle variations in the behavior of the
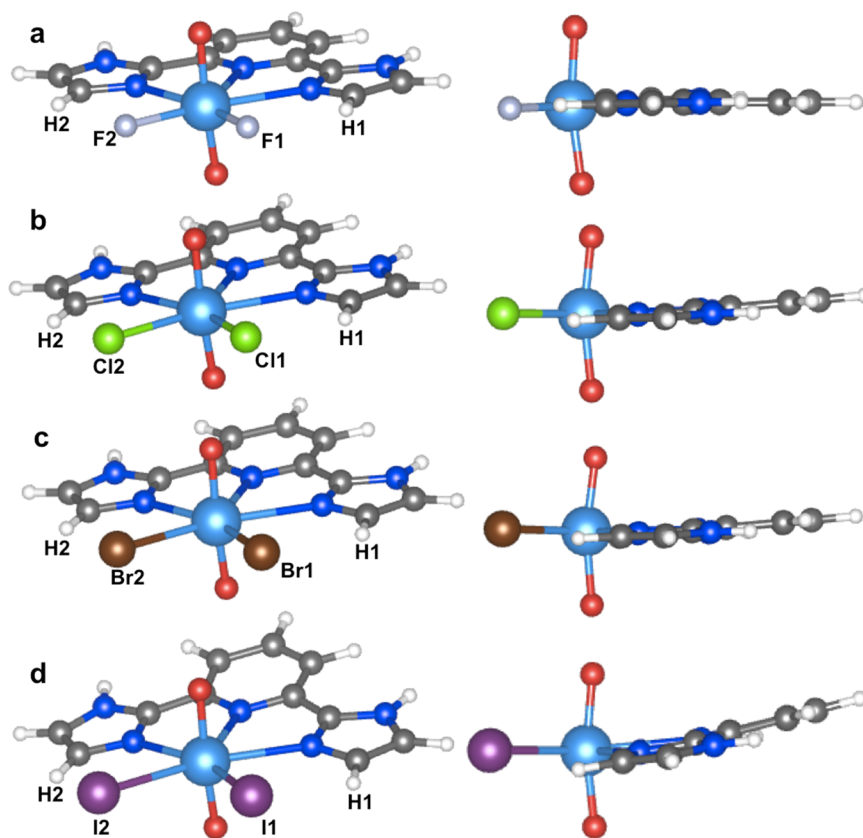
Figure 5. Structural models of isolated molecular units derived from complex 1 by truncating the benzene rings on the benzimidazole groups of the BBP ligand and substituting various halide ligands (a) F⁻, (b) Cl⁻, (c) Br⁻, and (d) I⁻ in the equatorial plane are shown. Side views of the complexes are shown on the right. For those atoms not explicitly labeled, the same labeling convention as used in Figure 2 is followed.

Table 4. GGA-Optimized Structural Parameters for Isolated Molecular Units Derived from Complex 1 by Truncating the Benzene Rings of the Benzimidazole Groups and Incorporating Different Halide Ligands Are Compared (See Figure 5)[a]

bond/angle	F [r_{ion} = 1.19 Å]	Cl [r_{ion} = 1.67 Å]	Br [r_{ion} = 1.82 Å]	I [r_{ion} = 2.06 Å]
U−O1	1.840	1.826	1.824	1.821
U−O2	1.840	1.826	1.824	1.822
U−N1	2.621	2.636	2.643	2.651
U−N2	2.806	2.776	2.765	2.750
U−N3	2.622	2.637	2.643	2.651
U−α1	2.142	2.621	2.791	3.035
U−α2	2.141	2.621	2.793	3.037
α1···H1	2.466 (2.09)	2.629 (2.57)	2.714 (2.72)	2.874 (2.96)
α2···H2	2.472 (2.09)	2.634 (2.57)	2.708 (2.72)	2.870 (2.96)
∠N1−N2−N3	113.1	114.1	114.5	114.7
∠N1−U−N3	120.1	121.5	122.0	122.1
∠α1−U−α2	95.6	86.7	84.4	81.8
∠Eq./N1N2N3	1.7	3.8	4.9	11.8

[a] In column 1, α1 and α2 represent the placeholders for the two halide ligand sites. The equatorial planes are generated by sets of three points, namely, α1, U, and α2. Units for distances and angles are angstroms and degrees, respectively. The numbers in parentheses indicate (r_{ion} + 0.9 Å).

planar structures, given that the same choice of the halide ligand yields equilibrium structures with very different nonplanar angles based on the size of the N-donor ligand, we are once again able to establish the primacy of steric effects and rule out halogen electronegativity differences, as being a significant factor in the structural trends observed across the series of halide ligand complexes. Our computational study shows that the structural properties of N-donor uranyl complexes are sensitive to both the effective charge states of the ligands and steric interactions and

can be systematically tuned by incorporating ligands of different sizes.

■ CONCLUSIONS

The structural properties of a series of uranyl complexes; $[(UO_2)(H_2BBP)Cl_2]$ (**1**), $[(UO)_2(HBBP)(Py)Cl]$ (**2**), and $[(UO_2)(BBP)(Py)_2]$ (**3**); based on the N-donor ligand 2,6-bis(2-benzimidazyl)pyridine (H_2BBP) are investigated theoretically with a particular emphasis on the nonplanarity observed in these complexes about the equatorial plane of uranyl. Through a

series of computational experiments, the role of different factors such as crystal packing, ligand electronegativity, and steric effects in driving the nonplanarity is explored. We find that the steric interaction between bulky halide ligands characterized by large ionic radii and nearby H groups on the benzimidazole groups of the BBP ligand is the primary reason for the nonplanarity and the role of other factors, such as axial uranyl distortions, is insignificant in this regard. Furthermore, these steric effects can be exploited to systematically tune the structural properties of these complexes by incorporating ligands of different sizes, and we believe this will be useful for the design of actinide complexes.

COMPUTATIONAL DETAILS

Electronic structure calculations were carried out using the DFT[25,26] platform provided by the Vienna ab initio simulation package,[27,28] which implements a planewave basis set framework in conjunction with projector augmented wave[29] pseudopotentials. The DFT exchange-correlation energy is modeled within the Perdew—Burke—Ernzerhof[30] GGA.[31] A planewave cutoff of 400 eV is used for the wave functions, and the Brillouin zone is sampled at the Γ point. As the uranium ion in $\{UO_2\}^{2+}$ features a nominally empty 5f shell in its U^{6+} oxidation state with an electronic configuration of $1s^22s^22p^63s^23p^3d^{10}4s^24p^64d^{10}4f^{14}5s^2$-$5p^65d^{10}6s^26p^6$, f-electrons do not play a significant role in the ground state electronic structure. Therefore, on-site Coulomb repulsion corrections are not employed in our structural analysis. Relativistic effects are taken into account within the core regions of the atoms in constructing the pseudopotentials employed but are neglected in the valence self-consistent field calculations. Supercells of the isolated complexes are constructed within a periodic boundary condition approach so that atoms in neighboring image cells are separated by at least 8 Å of vacuum, and the Brillouin zone is sampled at the zone center. Geometry optimizations are carried out until all forces are smaller than 0.01 eV/Å. Structural models shown were created using the VESTA-3[32] program.

AUTHOR INFORMATION

Corresponding Author
*E-mail: scpemmaraju@lbl.gov.
ORCID ⊙
Chaitanya Das Pemmaraju: 0000-0002-9016-7044

Notes
The authors declare no competing financial interest.

ACKNOWLEDGMENTS

REFERENCES

(1) Choppin, G.; Liljenzin, J.-O.; Rydberg, J.; Ekberg, C.; Choppin, G.; Liljenzin, J.-O.; Rydberg, J.; Ekberg, C. Chapter 21 — The Nuclear Fuel Cycle. In *Radiochemistry and Nuclear Chemistry*; Academic Press, 2013; pp 685−751.

(2) Hill, C. Overview of Recent Advances in An(III)/Ln(III) Separation by Solvent Extraction. In *Ion Exchange and Solvent Extraction*; CRC Press, 2009; pp 119−193.

(3) Drew, M. G. B.; Hill, C.; Hudson, M. J.; Iveson, P. B.; Madic, C.; Vaillant, L.; Youngs, T. G. A. Separation of Lanthanides and Actinides(iii) Using Tridentate Benzimidazole, Benzoxazole and Benzothiazole Ligands. *New J. Chem.* **2004**, *28*, 462.

(4) Escande, A.; Guénée, L.; Buchwalder, K.-L.; Piguet, C. Complexation of Trivalent Lanthanides with Planar Tridentate Aromatic Ligands Tuned by Counteranions and Steric Constraints. *Inorg. Chem.* **2009**, *48*, 1132−1147.

(5) Muller, G.; Bünzli, J.-C. G.; Schenk, K. J.; Piguet, C.; Hopfgartner, G. Influence of Bulky N-Substituents on the Formation of Lanthanide Triple Helical Complexes with a Ligand Derived from Bis-(benzimidazole)pyridine: Structural and Thermodynamic Evidence. *Inorg. Chem.* **2001**, *40*, 2642−2651.

(6) Petoud, S.; Bünzli, J.-C. G.; Glanzman, T.; Piguet, C.; Xiang, Q.; Thummel, R. P. Influence of Charge-Transfer States on the Eu(III) Luminescence in Mononuclear Triple Helical Complexes with Tridentate Aromatic Ligands. *J. Lumin.* **1999**, *82*, 69−79.

(7) Petoud, S.; Bünzli, J.-C. G.; Schenk, K. J.; Piguet, C. Luminescent Properties of Lanthanide Nitrato Complexes with Substituted Bis-(benzimidazolyl)pyridines. *Inorg. Chem.* **1997**, *36*, 1345−1353.

(8) Piguet, C.; Buenzli, J. C. G.; Bernardinelli, G.; Hopfgartner, G.; Williams, A. F. Self-Assembly and Photophysical Properties of Lanthanide Dinuclear Triple-Helical Complexes. *J. Am. Chem. Soc.* **1993**, *115*, 8197−8206.

(9) Kolarik, Z. Complexation and Separation of lanthanides(III) and actinides(III) by Heterocyclic N-Donors in Solutions. *Chem. Rev.* **2008**, *108*, 4208−4252.

(10) Copping, R.; Jeon, B.; Pemmaraju, C. D.; Wang, S.; Teat, S. J.; Janousch, M.; Tyliszczak, T.; Canning, A.; Grønbech-Jensen, N.; Prendergast, D.; Shuh, D. K. Toward Equatorial Planarity about Uranyl: Synthesis and Structure of Tridentate Nitrogen-Donor $\{UO2\}(2+)$ Complexes. *Inorg. Chem.* **2014**, *53*, 2506−2515.

(11) Pemmaraju, C. D.; Copping, R.; Wang, S.; Janousch, M.; Teat, S. J.; Tyliszcak, T.; Canning, A.; Shuh, D. K.; Prendergast, D. Bonding and Charge Transfer in Nitrogen-Donor Uranyl Complexes: Insights from NEXAFS Spectra. *Inorg. Chem.* **2014**, *53*, 11415−11425.

(12) Sessler, J. L.; Melfi, P. J.; Pantos, G. D. Uranium Complexes of Multidentate N-Donor Ligands. *Coord. Chem. Rev.* **2006**, *250*, 816−843.

(13) Wilkerson, M. P.; Burns, C. J.; Morris, D. E.; Paine, R.T.; Scott, B. L. Steric Control of Substituted Phenoxide Ligands on Product Structures of Uranyl Aryloxide Complexes. *Inorg. Chem.* **2002**, *41*, 3110−3120.

(14) Sarsfield, M. J.; Steele, H.; Helliwell, M.; Teat, S. J. Uranyl Bis-Iminophosphorane Complexes with in- and out-of-Plane Equatorial Coordination. *Dalton Trans.* **2003**, 3443.

(15) Sarsfield, M.J.; Helliwell, M.; Raftery, J. Distorted Equatorial Coordination Environments and Weakening of UO Bonds in Uranyl Complexes Containing NCN and NPN Ligands. *Inorg. Chem.* **2004**, *43*, 3170−3179.

(16) Arnold, P. L.; Pécharman, A.-F.; Hollis, E.; Yahia, A.; Maron, L.; Parsons, S.; Love, J. B. Uranyl Oxo Activation and Functionalization by Metal Cation Coordination. *Nat. Chem.* **2010**, *2*, 1056−1061.

(17) Pedrick, E. A.; Wu, G.; Kaltsoyannis, N.; Hayton, T. W. Reductive Silylation of a Uranyl Dibenzoylmethanate Complex: An Example of Controlled Uranyl Oxo Ligand Cleavage. *Chem. Sci.* **2014**, *5*, 3204−3213.

(18) Lu, E.; Cooper, O. J.; McMaster, J.; Tuna, F.; McInnes, E. J. L.; Lewis, W.; Blake, A. J.; Liddle, S. T. Synthesis, Characterization, and Reactivity of a Uranium(VI) Carbene Imido Oxo Complex. *Angew. Chem., Int. Ed.* **2014**, *53*, 6696−6700.

(19) Kiernicki, J. J.; Cladis, D. P.; Fanwick, P. E.; Zeller, M.; Bart, S. C. Synthesis, Characterization, and Stoichiometric U−O Bond Scission in Uranyl Species Supported by Pyridine(diimine) Ligand Radicals. *J. Am. Chem. Soc.* **2015**, *137*, 11115−11125.

(20) Maynadié, J.; Berthet, J.-C.; Thuéry, P.; Ephritikhine, M. The First Cyclopentadienyl Complex of Uranyl. *Chem. Commun.* **2007**, 486−488.

(21) Seaman, L. A.; Pedrick, E. A.; Tsuchiya, T.; Wu, G.; Jakubikova, E.; Hayton, T. W. Comparison of the Reactivity of 2-Li-C$_6$H$_4$CH$_2$NMe$_2$ with MCl$_4$ (M = Th, U): Isolation of a Thorium Aryl Complex or a Uranium Benzyne Complex. *Angew. Chem., Int. Ed.* **2013**, *52*, 10589−10592.

(22) Pedrick, E. A.; Schultz, J. W.; Wu, G.; Mirica, L. M.; Hayton, T. W. Perturbation of the O−U−O Angle in Uranyl by Coordination to a 12-Membered Macrocycle. *Inorg. Chem.* **2016**, *55*, 5693−5701.

(23) Berthet, J.-C.; Nierlich, M.; Ephritikhine, M. A Novel Coordination Geometry for the Uranyl Ion. Rhombohedral Uranium Environment in [UO2(OTf)2(bpy)2] and [UO2(phen)3][OTf]2. *Chem. Commun.* **2003**, *132*, 1660.

(24) Berthet, J.-C.; Nierlich, M.; Ephritikhine, M. Oxygen and Nitrogen Lewis Base Adducts of [UO2(OTf)2]. Crystal Structures of Polypyridine Complexes with out-of-Plane Uranyl Equatorial Coordination. *Dalton Trans.* **2004**, *76*, 2814.

(25) Hohenberg, P.; Kohn, W. Inhomogeneous Electron Gas. *Phys. Rev.* **1964**, *136*, B864−B871.

(26) Kohn, W.; Sham, L. J. Self-Consistent Equations Including Exchange and Correlation Effects. *Phys. Rev.* **1965**, *140*, A1133−A1138.

(27) Kresse, G.; Furthmüller, J. Efficient Iterative Schemes for Ab Initio Total-Energy Calculations Using a Plane-Wave Basis Set. *Phys. Rev. B: Condens. Matter Mater. Phys.* **1996**, *54*, 11169−11186.

(28) Kresse, G.; Furthmüller, J. Efficiency of Ab-Initio Total Energy Calculations for Metals and Semiconductors Using a Plane-Wave Basis Set. *Comput. Mater. Sci.* **1996**, *6*, 15−50.

(29) Blöchl, P. E. Projector Augmented-Wave Method. *Phys. Rev. B: Condens. Matter Mater. Phys.* **1994**, *50*, 17953−17979.

(30) Perdew, J. P.; Burke, K.; Ernzerhof, M. Generalized Gradient Approximation Made Simple. *Phys. Rev. Lett.* **1996**, *77*, 3865−3868.

(31) Parr, R. G.; Yang, W. *Density-Functional Theory of Atoms and Molecules*; Oxford University Press: New York, 1989; Vol. *16*.

(32) Momma, K.; Izumi, F. VESTA 3 for Three-Dimensional Visualization of Crystal, Volumetric and Morphology Data. *J. Appl. Crystallogr.* **2011**, *44*, 1272−1276.